Effect of Strain Rate on the Piastic Deformation in Aluminium Single Crystals

AUTHOR(S):

NISHIMURA, Hideo; TAKAMURA, Jin-ichi

CITATION:

NISHIMURA, Hideo ...[et al]. Effect of Strain Rate on the Piastic Deformation in Aluminium Single Crystals. Memoirs of the Faculty of Engineering, Kyoto University 1951, 13(1): 1-20

ISSUE DATE:

1951-01-31

URL:

http://hdl.handle.net/2433/280223

Effect of Strain Rate on the Plastic Deformation in Aluminium Single Crystals*

By

Hideo NISHIMURA and Jin-ichi TAKAMURA

(Received October, 1950)

Introduction

The most easily detected phenomenon in the plastically deformed crystal is the process of slip. This is characterized by the irreversible motion of one part of a crystal relative to another along a definite crystallographic plane. This motion is made evident by the appearance of bands on the surface of the specimen which correspond to the intersection of the slip planes with the surface. In a perfect crystal lattice, all parallel lattice planes are equivalent, but in practice slip takes place mainly on certain selected planes of a parallel system, giving rise to the well-known system of markings known as slip bands. These slip bands are commonly believed to play an important rôle in the deformation process. Most attractive theories in explanation of the slip process have been proposed by Becker, Orowan, Polanyi, Taylor and Burgers[1-5]. Experimental evidences of the direct kinds in explanation of the slip process, especially submicroscopic behaviors, are yet to be surveyed. Why are slip bands separated by finite distance and why does definite slip band occur? What has an important influence on the spacing between slip bands and the breadth of slip band? Does submicroscopic slip occur in the region between the obvious slip bands known as "glide packet"? If so, it may be said that there is an intimate connection between slip and creep. One of the distinguishing features of the slip process is the production of slip bands, so that if the process occuring during slip and creep were identical in any given case we might expect to establish this by observing slip bands in a specimen that has undergone creep. Chalmers[6] has found with tin at room temperature that creep occurs under the smallest stresses

* This paper was read on April 2nd, 1950 at the Spring Meeting of the Institute of Metals of Japan.

without any microscopic slip band. But it is most probable that slip bands occured in Chalmers' experiments were not resolvable in an optical microscope because of the small elongation [7]. Valuable results of submicroscopic gliding have been obtained by Heidenreich [8] and Brown [9].

The time element in the behavior of plastic gliding is one of the great difficulties encountered in systematizing the experimental results. As generally accepted, an increase in the strain rate, or rate of loading, acts in the opposite direction to increasing the temperature. The present investigation, therefore, has been carried out by electron-microscope to study the phenomena of plastic deformation in the crystallographically-same-orientated aluminium single crystals subjected to various strain rates at the room temperature. In this paper, the effect of strain rate on the slip bands behavior has been mainly discussed.

Striking differences in the width of slip bands, the number of sets of the slipped planes, the spacings between slip bands and the streaking of Laue spots (X-ray asterism) were observed between the crystals subjected to the slow rate of strain in the order of creep and the relatively rapid rate of strain. Another interesting fact was that the submicroscopic slip occured in the microscopic inter-slip region. The specimen which indicated the remarkable differences stated above, had such a crystallographic orientation that is not expected to exhibit double gliding until a very large extension has occured.

Experimental Methods

Aluminium single crystals of 99.9% purity, except the test specimen No. 12 of which purity is 99.6%, produced by the strain-annealing method, were at first electrolytically polished in a phosphoric acid solution without any preliminary mechanical polishing which is said to disturb the structure to a depth attaining about 20μ for the single crystal of aluminium [10]. Each single crystal was divided into two or three parts so that sach part may be more than 50mm long. Then each part was subjected to the extension of various rates of loading. The specimens were deformed at an approximately constant rate of loading of water at the room temperature. Oxide film on the surface produced by electrolytic polishing would be broken up along the slip band as the plastic gliding commences. Then the specimen was anodically oxidized in an ammonia-borax basic solution*. The oxide films, thus obtained, were peeled off in a mercuric chloride solution. These oxide film replicas were observed in an electron-microscope.

* This solution is composed of 28% ammonia water and the equal volume of the aqueous solution of 0.05 mol borax.

Using this method, the slip bands were observed clearly as in Photo. 1. The white band is the slip band and the net-work structure is the non-glided part. By increasing the time of anodic oxidation, we can obtain the different image of the slip band as shown in Photo. 2. From these electron images we can recognize that the increase of the thickness of oxide film produced by anodic oxidation occurs chiefly at the slip band, because the gliding place has no oxide film and the non-gliding part has already the primary oxide film produced by electrolytic polishing. These white and black images of slip bands, therefore, are formed according to the change of thickness of the oxide films produced by anodic oxidation. As in photo. 2, slip band shows the black

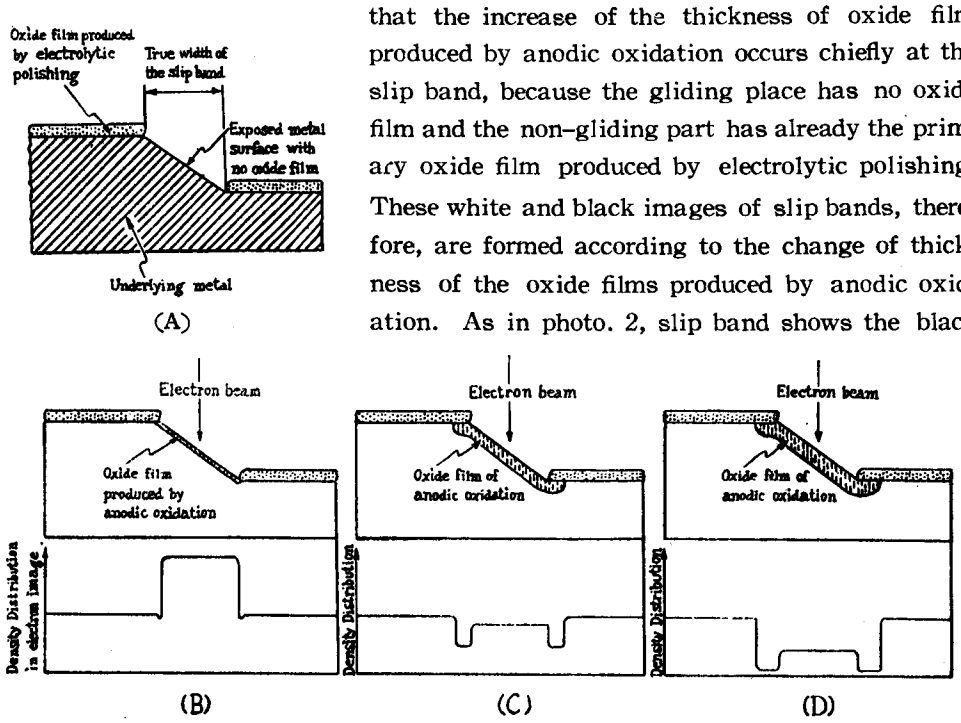

Fig. 1. Preparation of the oxide replicas for use in an electron-microscope.
(A) illustrates the slipped state of crystal and (B) (C) (D) indicate the change of density distribution in electron image caused by increasing the time of anodic oxidation. The time of anodic oxidation of (B) is less than 15 seconds (terminal voltage 12 V), (C) less than 30 seconds and (D) is more than 30 seconds.

parts on both edges. The black parts do not appear within a critical time of anodic oxidation (Photo. 1), but they could be observed with the increase of the time of anodic oxidation. An increase in the time of anodic oxidation acts in the direction to broadening the breadth of black edge. It may be said consequently that the black edges of the slip bands are formed in such a way as illustrated in Fig. 1. In this picture, Fig. 1-B shows the anodic oxidation in the shortest time; Fig. 1-C, that of the longer period; and Fig. 1-D, that of the longest period. Photo. 1 and 2 correspond respectively to Fig. 1-B and 1-D. Namely the appearance of the black edges can be interpreted as the superposing of two kinds of oxide films; the one is produced by electrolytic polishing and the other by anodic oxidation. The difference of the texture between two kinds

of oxide films at the slip band and the non-glided part is seen in Photo. 3. Therefore, the true breadth of the slip band is given as shown in Fig. 1-B. Using this method, the breadth of the slip band is measured with the accuracy down to 200 Å or less than that. If any defect was produced in the oxide film during deformation, a black spot would be observed by anodic oxidation in the same manner as illustrated in Fig. (1-B)~(1-D). Taking place any slip which is too slight to be resolvable in an electron image, the oxide film would be broken up at the slipped place. And so by increasing the time of anodic oxidation, we can observe the slight slip regions distinctly. The black spots and rods in photo. 3 mean the existence of such slight slip regions. These images, however, were not observed in the oxide replica of the specimen prepared in the same manner as Fig. 1-D which was not subjected to any plastic deformation. Accordingly we can illustrate the reason for attributing such black spots and rods to the occurence of the defects in the oxide film produced during plastic gliding.

The electron image of oxide replica has the direct relation to the thickness of replica. For the specimen thickness normally encountered in electron microscopy, the relative intensity of the radiation entering the objective from different points of the object is given by the following equation [11]:

$$\frac{I}{I_0} = e^{-N\sigma x}$$

where σ is the cross section for single scattering through the angles greater than the physical objective aperture, N the number of atoms per cm^2 with cross section σ and x is the thickness of the replica at the point in question. Accordingly when the metal has any curved surface, the blackening of the electron image of of the oxide replica peeled from the surface of the specimen would change gradually, provided the thickness of the oxide film is approximately uniform. This fact is observed in Photo. 4.

The slope of the surface of the test specimen resulting from the deformation, was measured directly by the stereographic analysis of the electron-micrographs. The specimens were also examined by X-ray before and after working in order to investigate the crystallographic orientations and the X-ray asterism.

Crystallographic Analyses of the Principal Specimens

The results of X-ray analyses of test specimens No. 32 and No. 40 are shown in Table I. Test specimens of 32 A and 32 B or 40 A and 40 B have respectively the same crystallographic orientations, since A and B are originated from a long plate of single crystal. Fig. 2 shows the projected pictures of the crystal lattics

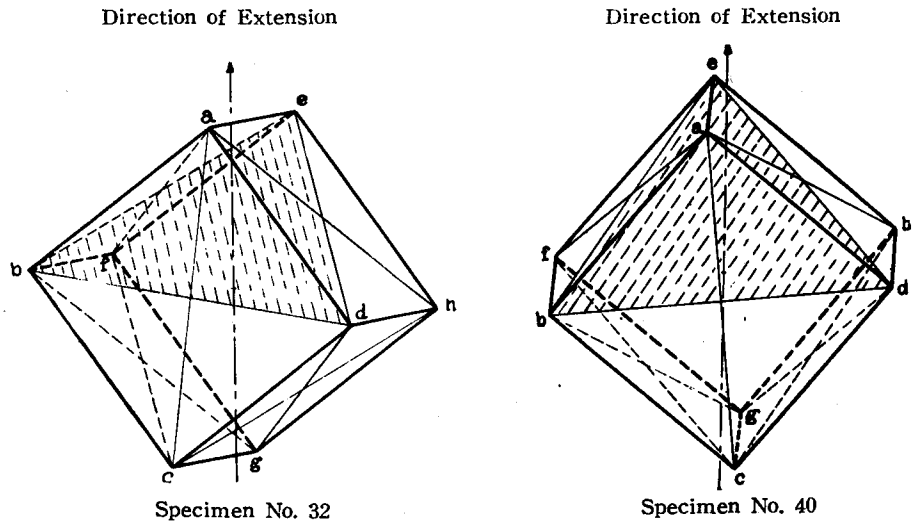

Fig. 2. Projection of the crystal lattice of the specimen to the surface of plate
Here,
(1 1 1)—△bde, (1 $\bar{1}$ $\bar{1}$)—△bdg, (1 1 $\bar{1}$)—△acf, (1 $\bar{1}$ 1)—△ach,
[0 1 1]—ac, [1 $\bar{1}$ 0]—de, [1 1 0]—bg, [1 0 $\bar{1}$]—be, [1 0 1]—dg.

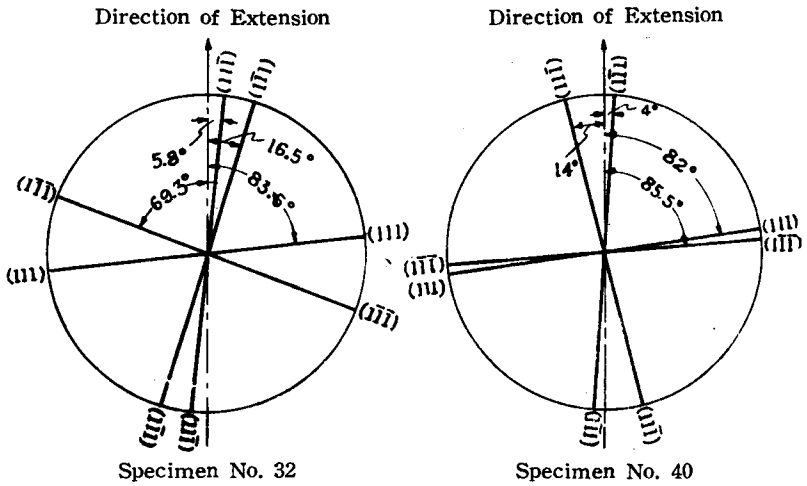

Fig. 3. Predicted directions of the traces of the {1 1 1} planes on the surface of the test specimen before extension

of the specimen on the surface of plate. From these pictures, many crystallographic relations are obtained quickly. Fig. 3 indicates the relation between the axis of the test specimen and the traces of the {1 1 1} slip planes on the surface of the plate. As shown in Table I, single slip on the (1 1 1) plane is

predicted up to 55.6% elongation in specimen No. 32 and 46.5% in No. 40. As soon as the axis of the test specimen reaches the boundary of the spherical triangle of stereo-projection, slip is to begin also on the $(1\bar{1}1)$ plane in specimen No. 32 and on the $(11\bar{1})$ plane in No. 40. This seems to be an ideal case in which the strain rate is extremely slow. For, as stated afterwards, the specimen

Table I

Specimen	Slip-plane	Direction of Slip	θ	λ	$\cos\theta\cdot\cos\lambda$	ε
No. 32	(111)	$[1\bar{1}0]$	41°	51°	0.474	55.6%
	$(1\bar{1}\bar{1})$	$[110]$	33°	58°	0.444	
	$(1\bar{1}1)$	$[011]$	80°	10°	0.170	
	$(11\bar{1})$	$[011]$	84°	10°	0.102	
No. 40	(111)	$[10\bar{1}]$	49°	46°	0.455	46.5%
	$(1\bar{1}\bar{1})$	$[101]$	22°	69°	0.332	
	$(11\bar{1})$	$[011]$	77°	15°	0.217	
	$(1\bar{1}1)$	$[011]$	87°	15°	0.050	

θ=Angle between the axis of the test piece and the normal to the slip plane. λ=Angle between the axis of the test piece and the direction of slip. ε=Elongation percentages calculated by the equation, $\cos\theta'=\cos\theta\cdot\varepsilon$. θ' is the value of θ when the test piece axis reaches the boundary of the spherical triangle of stereo-projection during the deformation.

subjected to the ordinary strain rate gives generally 2–4 sets of slip bands on the surface of the specimen within the area of single slip as predicted in the generalization of Taylor and Elam [12].

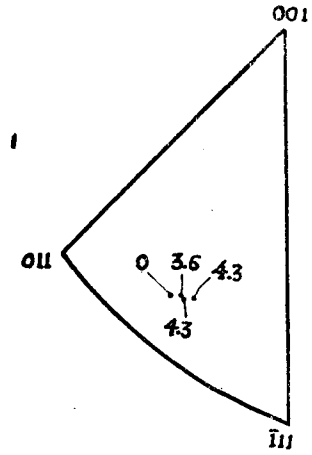

Fig. 4. Movement of test-piece axis relative to crystal axes. Numbers on top refer to measured elongation in %. Numbers underneath refer to calculated.

Conditions of Extension of the Main Specimens

Conditions of extension are given in Table II. As previously described, the test specimens were stretched by the continuous loading of water without any abrupt change of loading. Initial load in Table II is the weight of the chuck and the other accessories hung at an end of the test specimen. Setting of the test specimen at the chuck was made with the greatest care without bending or twisting. Fig. 4 shows a stereo-projection of the movement of the axes of the

test specimens No. 40 A and B in relation to the crystal axes. In this figure we can observe that in the initial stage of extension, the reorientations measured from the X-ray data exceed the calculated value.

Table II

Specimen	Initial load (g/mm^2)	Loading rate ($g/mm^2/sec$)	Total load (g/mm^2)	Elongation (%)	Active gliding plane
32A	15.10	0.0126	1014.12	8.67	(1 1 1)
32B	15.43	5.8256	1060.46	7.53	(1 1 1), (1 $\bar{1}$ $\bar{1}$)
40A	19.20	0.0305	958.55	4.35	(1 1 1)
40B	19.20	56.8730	833.53	3.65	(1 1 1), (1 $\bar{1}$ $\bar{1}$) (1 $\bar{1}$ 1), (1 1 $\bar{1}$)

Results and Discussion

It is made evident by the stereographic analyses of the electron-micrographs, as described afterward, whether the electron images of the bands obtained by our method truly indicate the slip bands or not. If these bands are the slip bands, they should have the slopes relative to the interslip region. Measuring the slopes of the bands, the bands really have the various slopes. Thus the bands observed by this method are the true slip bands. It is well known that the anodic treatment of aluminium can produce oxide films on the surface. Roscoe [13] has found that the oxide film of Cadmium increases its critical shear stress. And Rehbinder (1947) has mentioned the surprizing effects that surface active agents will produce in the resistance to plastic deformation. Therefore, the oxide film of the surface of metal seems to have an important influence on the plastic gliding. The results obtained in this experiment, however, would suggest a certain tendency of the plastic behavior of the underlying aluminium single crystals.

1. Breadth of the slip bands and spacings between the slip bands.

In the first place, the striking differences between test specimen 40 A and 40 B are the breadth of the slip bands and the spacings between slip bands as shown in the electron-micrographs of Photo. 5 and 6. This is similar to the differrence between the test specimen No. 32 A and 32 B (Photo. 8 and 9). A specimen subjected to a slow rate of strain generally has the wider slip bands and the wider spacings than that of a rapid strain rate. As an increase in speed of testing affects the plastic gliding behavior in much the same manner as a decrease in temperature, the results stated above seem to agree with the fact

that the spacing increases with increasing temperature [9] [14]. Photo. 10 shows a bundle of the fine parallel slip bands (narrow glide lamellae) in specimen No. 20 which appears to be a band in an optical microscope. This specimen had nearly the same crystallographic orientation as the specimen No. 40 and it was subjected to the rapid rate of strain of about 1% per sec., stretching to 5.2% total elongation. A bundle of these narrow glide lamellae in the specimen subjected to a rapid extension seems to correspond to a wide slip band in the specimen for a slow extension. It is interesting that such "lamellae gliding" occured also in the specimen subjected to a slow extension as shown in Photo. 11 and 12. But there are great differences of the breadth of slip bands and the thickness of the glide packets between in the specimen subjected to a slow rate of strain and a rapid rate of strain. As observed in Photo. 5, new slip bands were born at the equal distance apart from the primary slip bands which appear to be wider bands in this photograph, at the initial stage of deformation in which the distortion of crystal is not so intense. But at the later stage of deformation slip bands are generated one after another at the part adjacent to the initial slip bands. Denoting the average number of slip bands per unit length on the surface of the specimen as N and the average breadth of the slip bands as D,

$$\gamma = N \cdot D, \qquad N = \frac{1}{\lambda}$$

where γ is the elongation, and λ the average spacing between slip bands. If the strain is definite, the breadth of the slip bands must be proportional to the spacing between slip bands. That is, a specimen which has the wider slip bands should have also the larger spacings between slip bands than a specimen with the narrow slip bands. The results obtained in an electron-microscope, as stated above, demonstrate this tendency qualitatively.

Impurities seem to have a serious effect on increasing the breadth of the slip bands. In specimen No. 12 whose crystallographic orientation is nearly the same as the specimen No. 32, the narrow slip bands such as in the specimen No. 20 B, 32 B, 40 B were not observed in spite of a rapid strain rate of the order of 10^{-1}% per sec.. The purity of test specimen No. 12 is 99.6% and those of specimens No. 20, 32, and 40 are 99.9%. This may be correlated to the effect of impurity in increasing the critical shear stress [14].

The softness of the single crystals can be accounted for in a way originally suggested by A. A. Grifith to explain the mechanical behaviour of glass threads, by assuming that the solid contains flaws of some kind which produce a large local concentration of stress, in virtue of what may be called the "notch effect". The shear within the glide lamella itself may have a very high value, as may

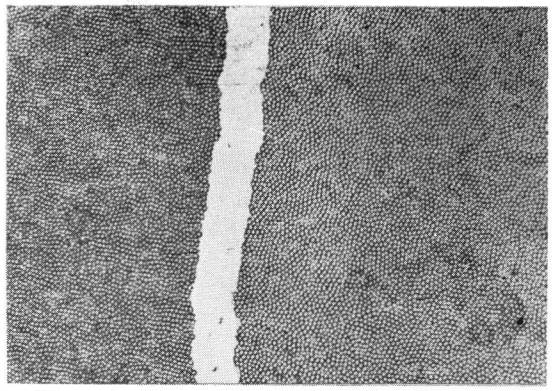

Photo. 1. Test specimen No. 32 A. White part is the sip band and the part with net-work structure is oxide film on the surface of specimen. Anodic oxidation time of this photograph is 14 seconds. 8,500×

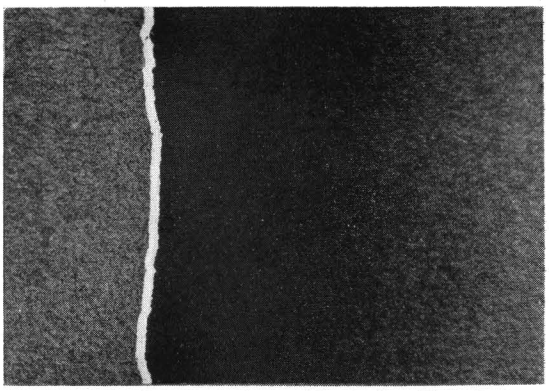

Photo. 4. Test specimen No. 40 A. The slope of the part adiacent to the slip band is shown by the intensity distribustion in electron image. 1,300×

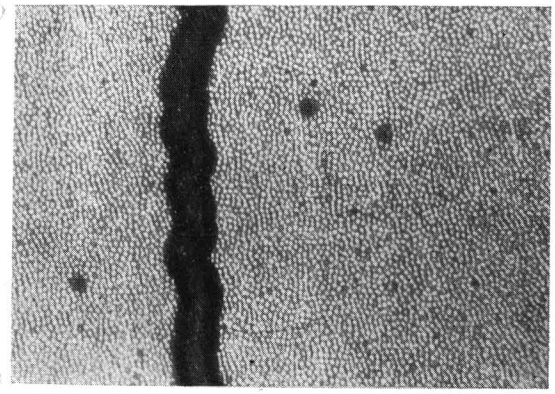

Photo. 2. Test specimen No. 32 A. The black edges on both sides of the slip band is formed as illustrated in Fig. 1. Anodic oxidation time is 32 seconds. 13,300×

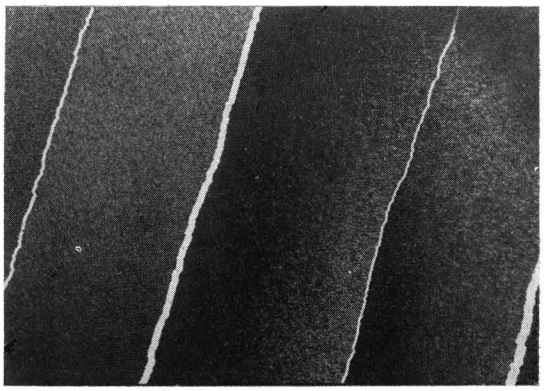

Photo. 5. Slip bands in the slowly deformed specimen No. 40 A. White are the slip bands 1,000×

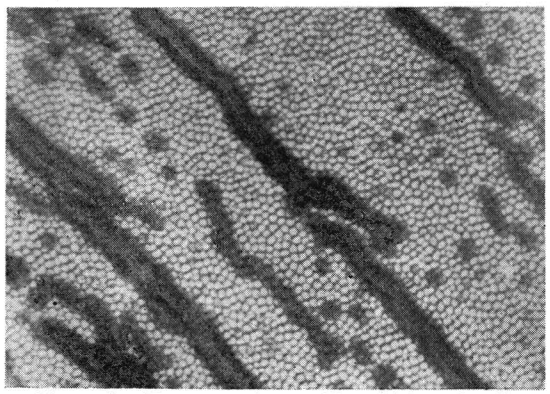

Photo. 3. Test specimen No. 34 A. Anodic oxidation time is 28 seconds. Superposing of two kinds of oxide films is well observed. 25,000×

Photo 6. Slip bands in the rapidly deformed specimen No. 40 B. Fine and short are the slip bands. 1,100×

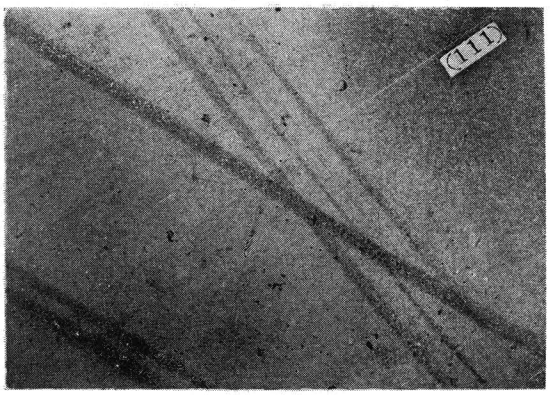

Photo. 7. Test specimen No. 40 B. Many sets of the slip bands are observed. 1,100×

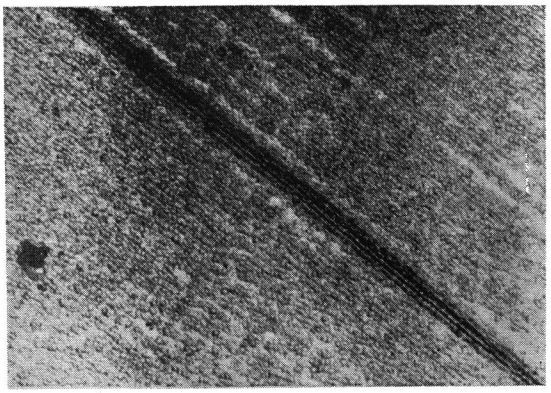

Photo. 10. Rapidly stretched specimen No. 20 B. Such lamellae gliding was found for the first time by Heidenreich and Schockley.[8] 13,000×

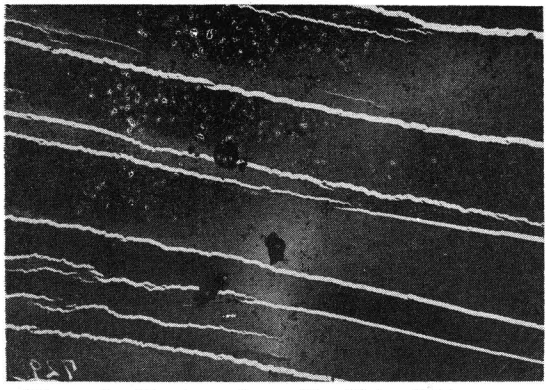

Photo. 8. Test specimen No. 32 A. White are the slip bands. This oxide film replica was extremly contaminated after setting on the holder. 1,000×

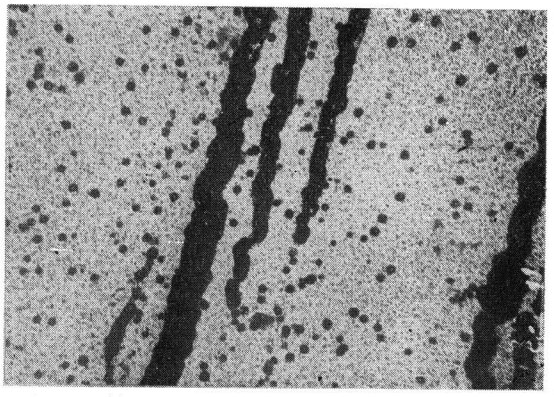

Photo. 11. Lamellae gliding of test specimen No. 32 A. Black bands are the slip bands and the black spots do not the contamination as illustrated in page 3. 4,600×

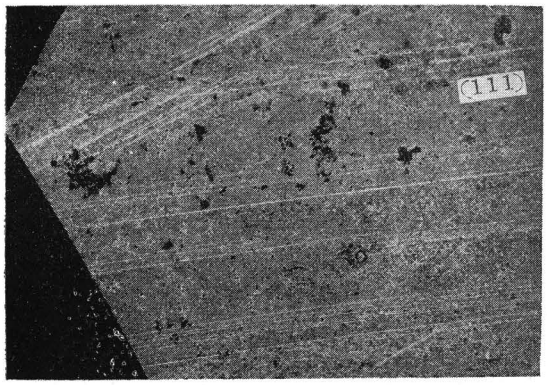

Photo. 9. Test specimen No. 32 B. Two sets of the slip bands are observed. The one is the (111) plane and the other is the $(1\bar{1}\bar{1})$ plane. 1,600×

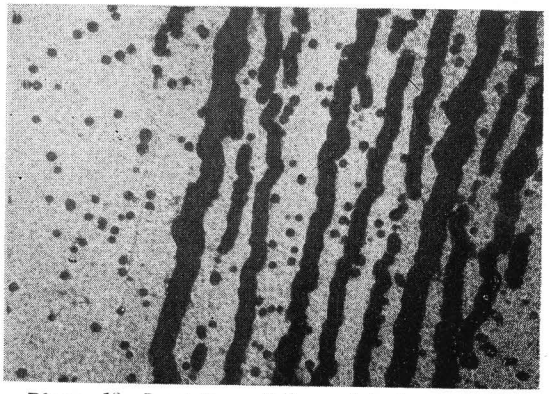

Photo. 12 Lamellae gliding of test specimen No. 32 A. Black bands and rods are the slip. See also photo. 10. 4,600×

be seen at once when we remember that the displacement on such a lamella, of extremly small thickness, may be sufficient to lay bare, in the direction of slip, a strip of the plane whose breadth is of the order of 0.5μ as in specimen No. 32 A and 40 A. Some of such slip bands were observed to have the breadth attaining about 1μ. On the contrary, in the specimen No. 32 B and 40 B subjected to a rapid rate of strain which showed the narrow breadth of the slip bands of the order of 0.1μ, the shear within the glide lamella itself may not have so much high value as in the specimen subjected to a slow rate of strain. These stress concentrations are considered to be at the edges of the dislocated area [15] of the glided planes.

2. Number of sets of the active gliding planes.

The second remarkable difference between them is the number of sets of the slip planes which are active in gliding. These sets of slip bands of each specimen observed in an electron-microscope are in Table II. Fig. 3 indicates the crystallographic analyses of the relation between the axis of the test specimen and the intersection of the $\{1\,1\,1\}$ slip planes with the surface of plate. Photo. 7 and 9 show the many sets of active gliding planes. Good identity will be found between Fig. 3 and Photo. 7 and 9. In these specimens single slip was predicted within the scores of percentages of elongation, as in Table I, nevertheless 32 B and 40 B showed many sets of slip bands as in these photographs, even within several percentages of elongation. On the contrary, in the specimen 32 A and 40 A, only one set of the slip bands of the $(1\,1\,1)$ plane appeared on the surface as predicted. In an optical microscope the third and fourth sets of the slip bands in the specimen 40 B, namely those of the $(1\,1\,\bar{1})$ and $(1\,\bar{1}\,1)$ planes were difficult to observe. Perhaps it is because the relative slope of the direction of slip on these planes is small to the surface of plate; the common $[0\,1\,1]$ direction of slip on these planes is in the slope of 14°10′ relative to the surface of the plate. The third and fourth sets of slip bands have the irregular spacings, and then they do not distribute uniformly in the field of vision of electron-microscope. Such an unpredicted appearance of many sets of slip bands occured easily in the specimen of higher purity, which indicates more distinctly to show the tendency of the severe plastic flow in the surface layer than the one of lower purity. And the "surface plastic flow", as stated afterwards, is recognized more severe in the specimen subjected to a rapid strain rate than the one for a slow rate of strain. It is difficult to have such a positive evidence that the unpredicted sets of slip bands are produced only in the surface layer of the specimen. The region belonging to these unpredicted slip planes, however, seems to be not so great in consideration of the "surface plastic flow".

If the rotation of crystal and the slip hardening did not take place during

deformation, slip would occur along each plane in succession when the shearing stress on each plane reaches the value S in the following formula,

$$S = T \cdot \cos\theta \cdot \cos\lambda$$

In this formula T is the load per unit sectional area and the value of $\cos\theta \cdot \cos\lambda$ of each plane is in Table I. As shown in Fig. 4, the motion of the axis of the specimen subjected to a slow strain rate is larger than that for a rapid rate. We may say, therefore, as follows; in the specimen subjected to such a rapid strain rate that the active motion of the axis is unable to follow the calculated, many sets of slip bands appear within the area of single slip described by Taylor and Elam.

3. Submicroscopic slips in the region between the obvious slip bands.

Why are slip bands separated by finite distances? This problem is important, because we are interested in explaining the origin of slip bands. The fact that such definite slip bands occur seems to imply that dislocations cannot be generated with equal ease at all points in the specimen and slip is highly localized in separate planar regions. On the other hand, it is natural to consider that the regions of the easiest nucleation are those where the most stress magnification occurs and a number of those regions of varing degrees of weakness where slip nuclei may be generated are distributed at random throughout the specimen. And so it may be said that a slip band occurs only if a number of very weak spots happen to lie very near in the same plane parallel to the slip plane. In this event, however, there is no reason that no slip occurs in the regions between slip bands. It is possible that submicroscopic slips take place within the regions between the obvious slip bands [7].

In an optical microscope the slip band of the specimen subjected to a rapid rate of strain appears to be an indistinct band which is found to be composed of many narrow glide lamellae by an electron-microscope, as previously described. Slip band of the specimen subjected to a slow loading, on the other hand, is observed by an optical microscope and also by an electron-microscope as a distinct and obvious band. In either specimen, to our interest, many slight slips have been detected by an electron-microscope within the region between the optical microscopic slip bands. Photo. 13 indicates the submicroscopic fine slip lines in the region between the obvious slip bands in specimen No. 20 B which was subjected to a rapid loading. Similar results were obtained in specimen No. 32 B and No. 40 B, but in these specimens the slip bands appear to be torn to short bands or pieces.

In also the specimen subjected to a slow loading the submicroscopic slips can

be observed in an electron-microscope, but they present somewhat different figures. Photo. 11, 12, 14 and 15 are the electron images obtained in such a way as illustrated in Fig. 1-D. Black rods and spots in these photgraphs indicate the existence of the slight slips during the deformation as above described. We call them as "short range slips". These short range slips are not observed at the initial stage of deformation, but they appear in the regions between the obvious slip bands at the later stage in which the crystal is severely distorted. Such a generation of the short range slips in the region between the slip bands may be correlated to the release of the concentrated stresses at the distorted and fragmentated mosaic blocks. These short range slips are generally distributed at random on the surface of the test specimen, but they grow up to a long range slip and form a obvious slip band in such a manner as threading their way through many short range slip regions as the deformation proceeds. This fact that submicroscopic slips occur may give an important key in explaining the origin and the formation of slip bands.

4. Stereographic analyses of the electron-micrographs.

The electron-microscopic stereographs were taken with a replica holder whose top plate can be tilted about an axis as in Fig. 5. We shall call an electron-micrograph as a photograph "horizontal" in the case of the top plate of the replica holder setting horizontal, and in the case of setting tilted, as a photograph "oblique". Namely a photograph "horizontal" is an image given by a perpendicular incident electron beam and photograph "oblique" is given by an obliquely incident beam. Determing the tilted angle θ and the direction of the maximum slope of the tilted angle which is perpendicular to the rotation axis[16], and denoting the distance between the origin O and the measuring point P on the photograph "horizontal" as OP which is in the direction of the maximum slope, the coordinate of the point P can be represented as:

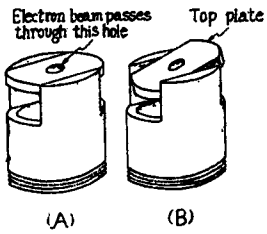

Fig. 5. Replica holder for the electron-microscopic stereographs (Hitachi-C. R. I.-type). (A) indicates the replica holder with a top plate setting horizontal and (B) setting tilted.

$$OP,\ \tan^{-1}(K\cdot\operatorname{cosec}\theta-\cot\theta)$$

where $K=\dfrac{O'P'}{OP}$ and the points O' and P' on the photograph "oblique" are the points corresponding to O and P on the photograph "horizontal".

From this calculation, the slope of the surface of the test specimen, i. e., the slope of the parts of slip band and the interslip parts on the surface, was

determined. Fig. 6 indicates the relation thus obtained between the slope of the slipped planes and the width of the slip bands on the surface of test specimen No. 12, whose purity was 99.6%. The slope and the width were measured in the direction of intersection on the surface of the test specimen with the plane which is prependicular to the surface and contains the crystallographic direction of slip. This result indicates that the slope of the slip band itself relative to the surface, i.e., the slope of the slipped plane resulting from plastic gliding on the surface, decreases with an increase in the width of the slip bands. Such decrease seemed to be more remarkable in the specimen of higher purity. Another result obtained by the stereographic analyses of electron-micrographs showed that the relative slope of the surface between slip bands produced during deformation was about

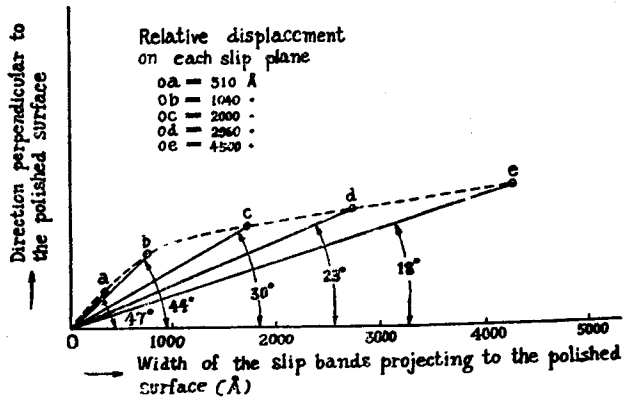

Fig. 6. Relation between the width of the slip band and the slope of the slipped plane relative to the polished surface in the direction of slip. The slope of the slip plane before extension was found to be 48° by X-ray analysis. The slope of the slipped plane was measured as the plane having no curvature. Calculation of the relative displacement on the slip plane was made on the basis of the width of the slip band and the slope of the slipped plane.

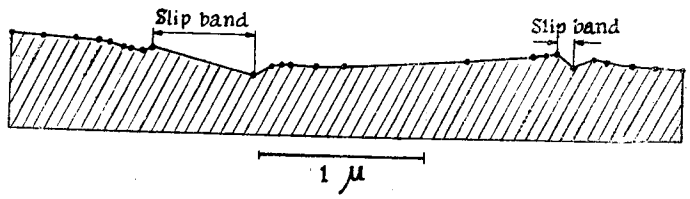

Fig. 7. A example of the perfect analyses of electron-microscopic stereographs. This picture indicates the slope of the surface neighbouring the slip bands in specimen No. 32 A.

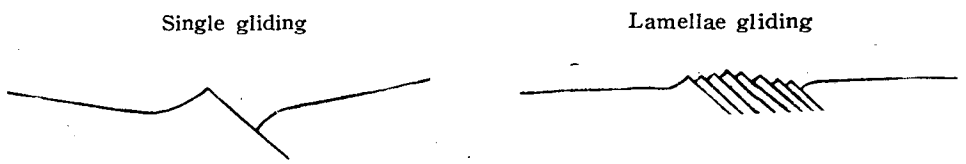

Fig. 8. Schematic pictures of slip process roughly sketched. Generally single gliding occurs in the slowly deformed specimen and lamellae gliding in the rapidly deformed one.

3–7° to the polished surface of plate in specimen No. 40 A, whose purity is 99.9%. This slope of the interslip part can be distinguished also by the change of blackening, as shown in Photo. 4 and 5. Each mearsuring points in Fig. 7 is in the direction of maximum slope of the stereographic rotation angle. From these results, we have obtained sachematic picture of slip process roughly sketched in Fig. 8.

5. Plastic flow in the surface layer of the specimen and X-ray asterism.

The Laue X-ray pattern of deformed crystal obtained by sending a beam of continuous radiation through the system, consists of radical streaks or bands instead of such sharp spots, as in an unstrained single crystal. This streaking is generally called asterism. A specimen deformed at a slow rate of strain generally gives rise to pronounced X-ray asterism than one subjected to rapid strain rate. And the rotation of the crystal measured by X-ray was larger in the former than in the latter. As previously described, a specimen subjected to a rapid strain rate has the wider slip bands and the larger spacings between slip bands and a larger number of sets of slip bands on the surface of the specimen than one for a slow rate of strain. Furthermore, the observation of the slip lines in test specimen No. 23 A and B stretched within 1% of total elongation, showed that each slip line which appeared on the top surface at the initial stage of deformation corresponds to the slip line on the back surface of the test specimen. Such correspondance of the number of slip lines on both surfaces decreases with an increase in strain rate and strain. Moreover, by the electron-microscopic observation of the behavior of mosaic blocks during deformation, the difference of fragmentation and distortion of mosaic blocks between the surface layer and the interior of test specimen has been recognized. These facts seem to imply that the plastic flow in the surface layer is more intense than in the interior of the specimen and the difference of plastic flow between at the surface layer and in the interior of the specimen increases with an increase in strain rate and strain.

It has been pointed out by a number of workers that the distortion of the Laue pattern can be explained by assuming that the bending of planes takes place about an axis lying in the slip plane and normal to slip direction. It is not possible to say whether or not this bending is accompanied by fragmentation. But we may say at least that the fragmention of the mosaic blocks in the region of slip occurs as shown in Photo. 16. Barret and Levenson [17] has suggested that the asterism may be connected with the occurance of the "deformation bands". In fact, the crystal is severely distorted at the region of the deformation bands, as shown in Photo. 17. This photograph indicates the distorsion of the slip bands at the deformation bands in test specimen No. 51 A which was deformed at the

slow rate of strain of 1.5×10^{-4}% per sec. and was stretched to 11.8% total elongation. The disorientation of the crystal at the part of deformation band is often detected by the chemical etching even after the restoration accompanied by no recrystallisation. Photo. 18 shows the disorientation of the crystal caused by the deformation bands in test specimen No. 20 after annealing at 525°C. Photo. 24 indicates the Laue pattern of the region of the deformation band in test specimen No. 61 which was deformed at the rate of strain of 6×10^{-4}% per sec. and was stretched to 5.5% total elongation. The spots in this pattern show the pronounced asterism and this asterism was found to be caused by the inverse rotation of crystal at the deformation band against the matrix crystal. The deformation bands, moreover, seem to be correlated to the division of the Laue spots.

Burgers [5] has pointed out that the warping of the lattice is directly connected with the presence of dislocations and when a large number of dislocation lines have been stopped at the warping region, the region may be able to show a rotation over a considerable angle. Considering the difference of the plastic flow in the surface layer and the difference of the breadth of slip bands between the specimens deformed at a slow strain rate and rapid strain rate, as stated above, the relative shift of the two regions into which the domain is seperated by the plane over which the dislocation lines move become large in the slowly deformed crystal than in the rapidly deformed crystal. It is conceivable that a large local stress concentration will appear at the head of an active gliding plane where the warping of the lattice occurs. The fact that a slowly deformed specimen gives rise to pronounced X-ray asterism than a rapidly strained specimen, may be understood that the stress concentration at the edge of an active gliding plane which causes the rotation of crystal is larger in the former than in the latter. Photo. 19 shows the joining figures of slip bands on the surface of the test specimen. In such joining parts also, the rotation of crystal may happen.

The conception given by Andrade [18] is that the rotation of crystallites does not take place in the glide lamellae but in the glide packets, for the asterism show that within the range of rotations the original orientation is not strongly preferred. The observation by the stereographic analysss and the change of blackening, as previously described, indicates that the slopes are produced during deformation in the interslip regions of the surface of the specimen. It is not possible to say, however, whether such slopes mean the rotation of crystallites in the glide packets. Another interesting fact is the shape of the end of the slip band on the surface observed in an electron-microscope. The end of the slip band has often such a shape as in Photo. 20. Such a shape may be interpreted as a result of the rotation of the crystal at that part about an axis normal to the slip plane.

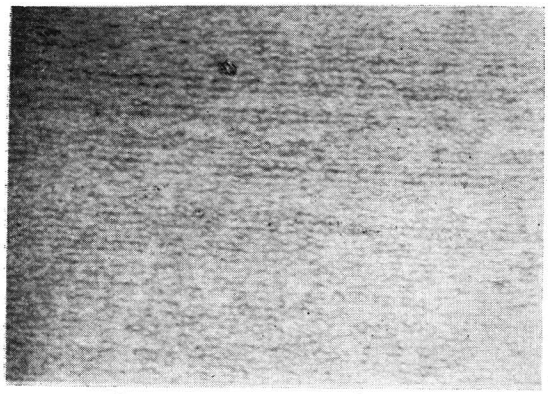

Photo. 13. Test specimen No. 20 B. Submicroscopic fiine slips in the region between the obvious slip bands. 23,000×

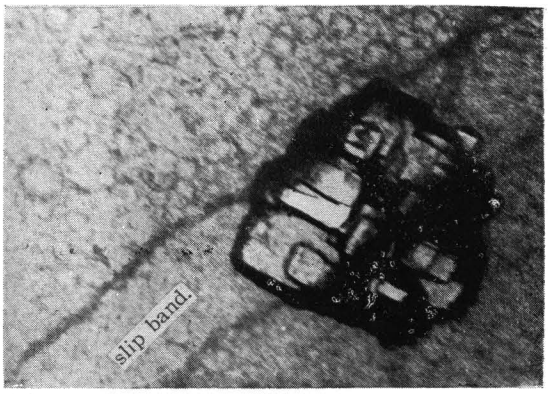

Photo. 16. Fragmentated mosaic blocks at the slip band, of test specimen No. 12. This image was obtained by etching after extension. 18,000×

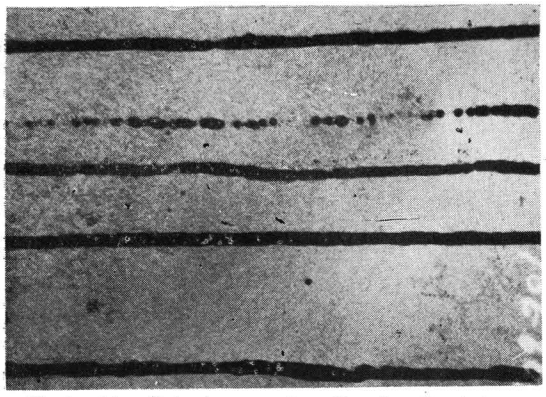

Photo. 14. Submicroscopic slips in the inter-slip region of test specimen No. 51 A. The time of anodic oxidation is 46 seconds. 2,600×

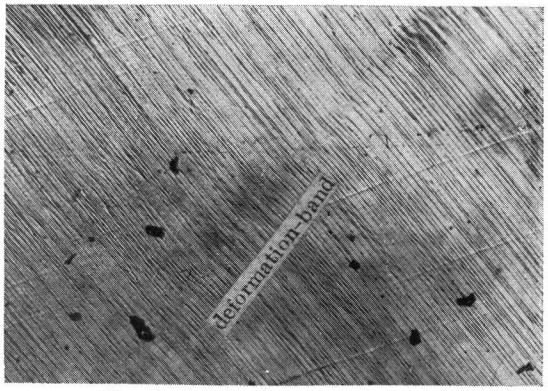

Photo. 17. Optical micrograph of test specimen No. 51 A. Two sets of slip bands and deformation band are observed. The first set of the slip bands is severely distorted by the deformation band. 77×

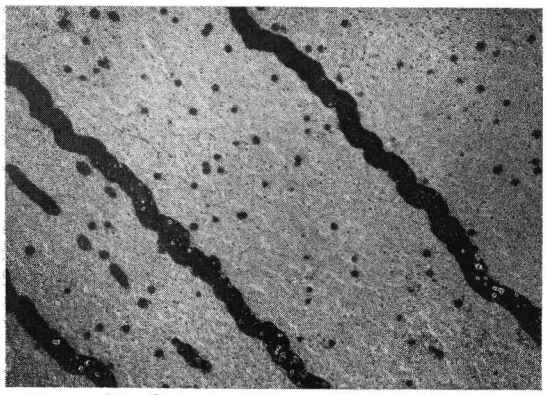

Photo. 15. Submicroscopic slips of test specimen No. 32 A. Black rods and spots are the short range slip regions (cf. Page 13). 4,600×

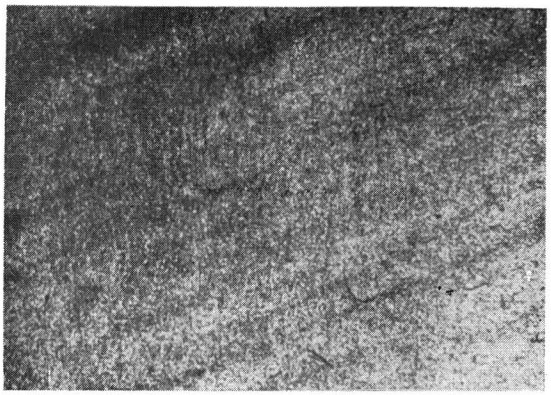

Photo. 18. Macro-texture after annealing at 525°C of test specimen No. 20 B. Many vague stripes of the disorientated regions caused by the deformation bands are observed. 6×

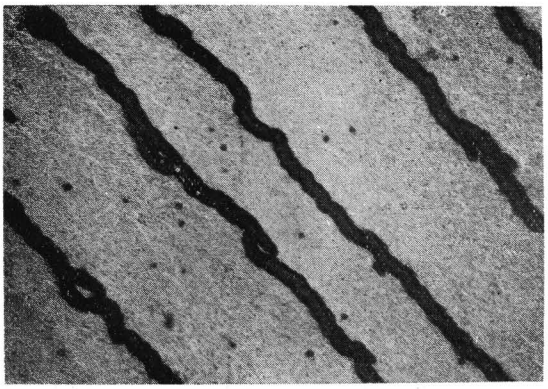

Photo. 19. Joining figures of the slip bands in test specimen No. 32 A. Black are the slip bands. 4,600×

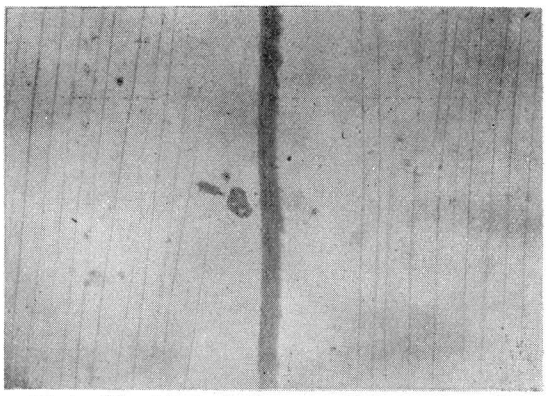

Photo. 22. Marked line parallel to the slip bands on the top surface of test specimen No. 40 A. The propagation of the slip has been hold up near the marked line. 77×

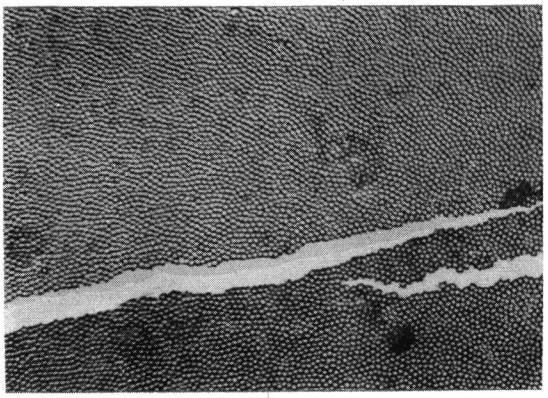

Photo. 20. Pointed shape of the ends of the slip bands of test specimen No. 32 A. White are the slip bands. 10,000×

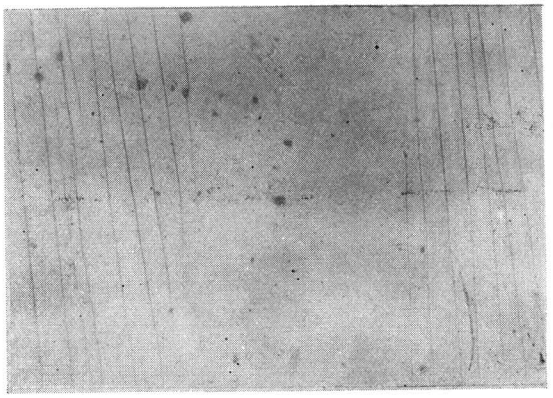

Photo. 23 Effect of the marked line of the top surface on the behavior of the slip bands of the back surface of test specimen No. 40A. 77×

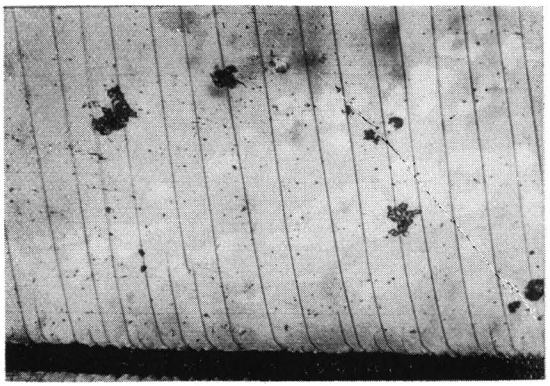

Photo. 21. Optical micrograph of test specimen No. 23. Black band underneath is the marked line perpendicular to the slip bands. 77×

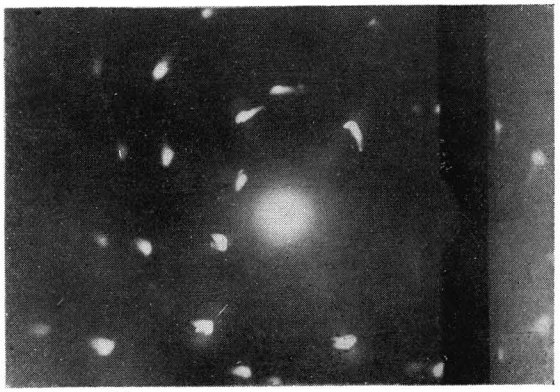

Photo. 24. Laue pattern of the region of the deformation band in test specimen No. 61.

Whether the rotation of the crystal about an axis normal to the slip plane and the slope produced during deformation which was detected by the stereographic analyses are directly connected with the X-ray asterism, has not yet been established.

From these results, we may say that the X-ray asterism is caused by the following different processes, namely: (1) the rotation of crystallites at the head of a active gliding plane (2) the bending of plane about an axis lying in the slip plane and normal to the slip direction (3) the rotation of crystallites at the deformation bands in the plane perpendicular to the active direction of slip (4) the rotation of crystal taken place in the glide packets (5) the rotation of crystallites about an axis normal to the slip plane.

6. Effect of the notch line of the surface on the behavior of the slip bands.

As regards the origin of the dislocation, it is believed that they are formed at the special spots with imperfections in the crystal where the stress is particularly high. These irregularities or defects in the crystal have two rôles — to make possible the formation of dislocations, and to hinder their motion. However, it is not clear that what influence on the motion of the dislocation the relative situation of the defects to the slip plane has. This problem seems to be connected with the effect of the grain boundary on the slip process. As it is difficult to investigate directly such problem, a convenient method was applied in the following manner. Fine straight line nearly parrallel, perpendicular and athwart to the predicted trace of the slip plane on the surface of the specimen, whose direction was beforehand determined by the crystal analysis, was marked on the electrolytically polished surface of the test specimen by the point of a needle. This fine straight line had the width and the depth of the order of about 10^{-2} mm, while the specimen plate was about 1,5 mm thick. The specimen with such a marked line was then stretched at the various rates of strain. The experimental results showed the following tendency regardless of the strain rate.

(a) In the case of perpendicular marked line to the slip bands, the slip bands were easily produced at the marked line on the surface. Photo. 2 indicates the slip bands neighbouring the marked line. (b) Parallel marked line to the slip bands on the surface of the test specimen gave a tendency to hold up the propagation of the slip and therefore slip bands were not observed at the neighbourhood of the marked line. And the non-slipped region was observed correspondently on the back surface of the plate, in spite of the absence of the marked line. Photo. 22 shows such region on the surface and Photo. 23 indicates the corresponding part on the back surface. (c) Marked line athwart to the slip bands did not indicate any important effect on the behavior of the slip bands.

Summary

A survey of the fine structures of slip bands in the electrolytically polished aluminium single crystals which were subjected to the extension of various loading rates was made by electron-microscope and X-ray. The results obtained were as follows; (1) The specimen subjected to a slow rate of strain generally shows the wider slip bands, the wider spacings between slip bands and the larger number of sets of the active gliding planes than the specimen subjected to a rapid strain rate. (2) The slowly deformed specimen generally gives rise to pronounced X-ray asterism and remarkable plastic flow in the surface layer than the rapidly deformed specimen. (3) Submicroscopic slips take place within the regions between the obvious slip bands. (4) The slopes of the surface of the test specimen produced during plastic deformation were determined by the stereographic analyses of the electron-micrographs. (5) Effect of the notch line of the surface on the behavior of the slip bands was observed.

Acknowledgement

The authors wish to thank heartily Dr. B. Tadano and Mr. S. Katagiri, Central Research Institude of Hitachi Work. Co., for their kindness and helps in taking electron-micrographs.

References

1) R. Becker, Physik. Zeits., **26** (1925) 919.
2) E. Orowan, Zeits. f. Physik, **89** (1934) 634.
3) M. Polanyi, Zeits. f. Physik, **89** (1934) 660.
4) G. I. Taylor, Proc. Roy. Soc., A. **145** (1934) 362, 388, 405.
5) J. M. Burgers, Proc. Phys. Soc., **52** (1940) 23.
6) B. Chalmers, Proc. Roy. Soc., **156** (1936) 427.
7) F. Seits and T. A. Read, J. App. Phys., **12** (1941) 100, 170, 470.
8) R. D. Heidenreich and W. Schockley, J. App. Phys., **18** (1947) 1029.
9) A. F. Brown, Nature, **163** (1949) 961.
10) J. Benard, P. Lacombe and G. Chaudron, Journe'es de Etates de surfaces, Oct. (1945) 73, Paris.
11) V. K. Zworkin, G. A. Morton, E. G. Ramberg, J. Hiller and A. W. Vance, Electron optics and electron-microscope (1945)
12) G. I. Taylor and C. F. Elam, Proc. Roy. Soc., A. **102** (1923) 643.
13) R. Roscoe, Phil. Mag., **21** (1936) 399.
14) E. N. DA C. Andrade and R. Roscoe, Proc. Phys. Soc., **49** (1937) 152.
15) E. Orowan, Proc. Phys. Soc., **52** (1940) 8.
16) H. Nishimura and J. Takamura, Report of the Comittee of the Electron-Microscopy of Japan, July (1950) 79.
17) C. S. Barret, Trans. A. I. M. E., **135** (1939) 296; C. S. Barret and L. H. Levenson, Trans. A. I. M. E., **135** (1939) 327.
18) E. N. DA C. Andrade, Proc. Phys. Soc., **52** (1940) 1.